Fine-Sediment Dispersal in the Gulf of San Miguel, Western Gulf of Panama: A Reconnaissance[1]

Donald J. P. Swift[2]

Marine Biology Group
Puerto Rico Nuclear Center
Mayaguez, Puerto Rico 00708

R. Gordon Pirie

University of Wisconsin at Milwaukee
Milwaukee, Wisconsin 53201

ABSTRACT

The Gulf of San Miguel, 30 km wide at its mouth and extending 40 km inland, is the estuary of river systems that drain eastern Panama. The Gulf consists of a central scour channel up to 36 m deep, flanked by semicircular bays. The tide has a range of up to 7 m, and maximum surface tidal currents average 200 cm/sec on the flood tide and 230 cm/sec on the ebb tide.

The water of the lower Gulf is weakly but uniformly stratified; in summer, surface salinities are 26 to 30 ppt while surface temperatures are close to 29°C; bottom salinities and temperatures are 2 to 3 units lower. In the upper Gulf and tributary estuaries, the proximity of fresh-water input, plus turbulence generated by the shoaling irregular bottom, results in a heterogeneous water structure. This structure varies sharply through time and space as salinity fronts form and are destroyed by turbulent mixing.

Shoal-water turbidity maxima in the mouths of tributary estuaries result from density-driven "estuarine" circulation. In addition, a turbid zone occurs around the margin of the Gulf proper. Surface turbidities of 60 to 200 mg/l are commonly observed shoreward of the 12-m isobath; turbidity seaward of this line is markedly lower and is mainly biogenic in nature. Turbidity develops over shoal areas as accelerating tidal currents generate a turbulent boundary layer and is associated with bed loads of clay slurry and clay gravels.

The size-frequency distributions of suspended sediments were measured *in situ* by means of a photoextinction turbidometer. Median hydraulic diameters show a direct correlation with depth and current velocity. Sediments resuspended as the tide floods across the shoals possess log-normal size-frequency distributions whose cumulative curves are straight lines on log-log plots. As the current strength wanes beyond the shoal, the distributions become coarse-truncated due to progressive loss of the coarse fractions.

Elements of the fine-sediment dispersal system include (i) input of fresh turbid water, (ii) a turbid stratified water mass, mainly occupying the central channel, (iii) thick prisms of

1. Accepted for publication and submitted to press 15 October 1969.
2. Present address: Institute of Oceanography, Old Dominion University, Norfolk, Virginia 23508.

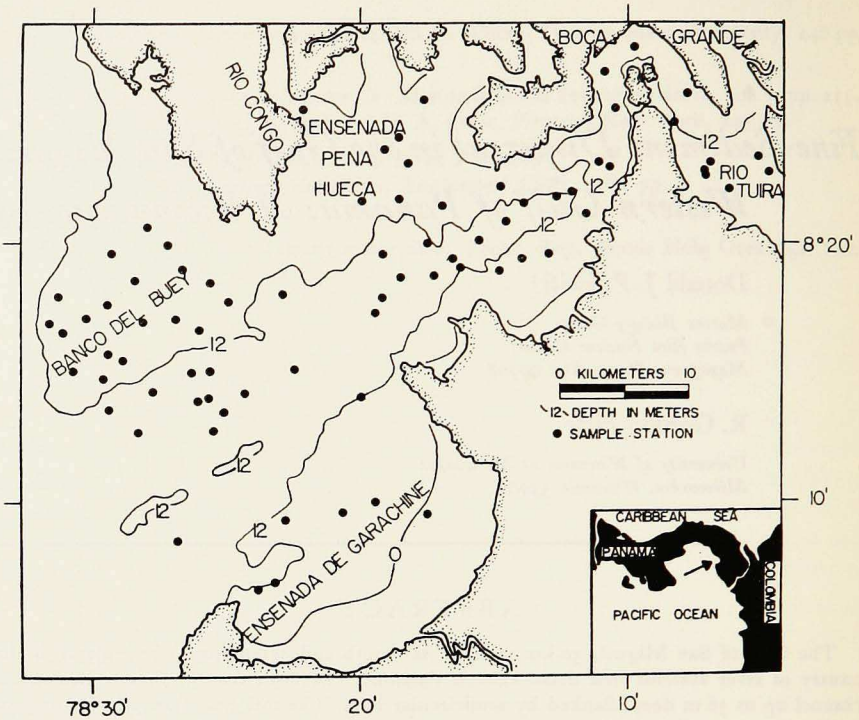

Figure 1. Sample net and location map.

lutite in the marginal bays, and (iv) turbid water output into the Gulf of Panama. The marginal prisms serve as mud reservoirs, which exchange material with the overlying water mass during every tidal cycle. They are not in equilibrium but are prograding toward the central channel.

Introduction. The Gulf of Panama (Fig. 1) is a northward extension of the Pacific Ocean, surrounded on three sides by the country of Panama. Its radius is about 100 km and it averages 50 m in depth. Its eastern shore is broken by a second-order embayment, the Gulf of San Miguel.

The Gulf of San Miguel is the Pacific terminus of one of the proposed routes for a new sea-level Panama Canal, to be dug with atomic explosives. This report is part of a larger study of the distribution and dispersion of trace elements on the Atlantic and Pacific coasts of Panama. The study was conducted by the Marine Biology Program, Puerto Rico Nuclear Center, Mayaguez, Puerto Rico, for Battelle Memorial Institute and the Atomic Energy Commission.

Field and Laboratory Methods. Field work was accomplished from July 2 to July 12, 1967, by the R/V Shimada, a 20-m coastal vessel. During the

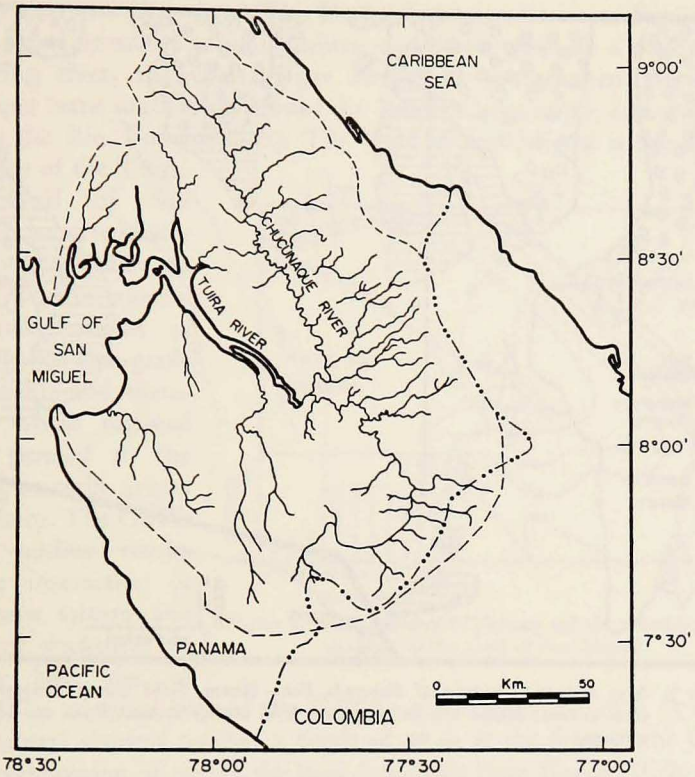

Figure 2. Drainage basin, Gulf of San Miguel (dashed line).

day, tidal water masses were tracked by means of a parachute drogue. The drogue consisted of a 25-kg lead weight connected by a 10-m nylon rope to a styrofoam float. A flag on a bamboo pole was attached to the float, and a parachute was attached by a bridle halfway down the nylon rope. While on drift station, we sampled the surface of the water mass every 15 minutes and the entire water column (at 1-m intervals) every half hour. Salinity, temperature, and conductivity were determined by means of an induction salinometer. Suspended-sediment samples were obtained with a continuous-flow centrifuge system as described by Jordan (1965). The turbidity of the water samples, bypassed by the system prior to centrifuging, was determined by means of a photoextinction turbidometer, modified from the design of Bradley (1956). The turbidometer was calibrated against standards prepared from local samples. Precision is estimated to be at least 0.01 mg/l in the range 0.02–2.00 mg/l. The same turbidometer was used to perform size analyses of suspended fine sediment within the 4-to-8-phi range, according to the techniques described by Simmons (1959) and McKenzie (1963). Since the particles observed were

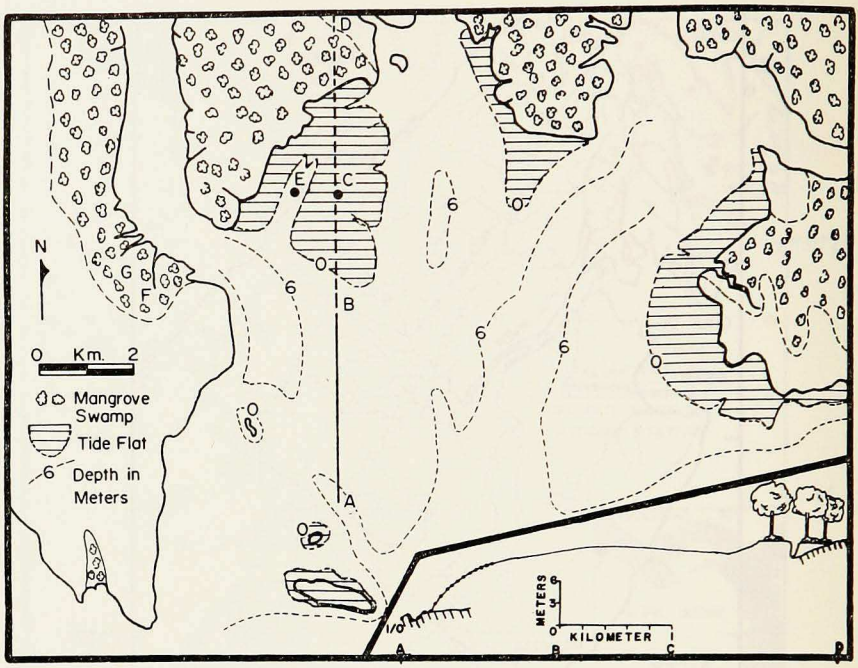

Figure 3. Map and cross section of Ensenada Pena Hueca. Solid line is measured portion of cross section; dashed line is estimated. E is anchor station. F, G are tidal-creek drift stations.

mainly suspended clay floccules rather than quartz grains, it was not possible to test the accuracy of the results by the microscope method. However, in uniformly dispersed samples that were free of neutrally buoyant vegetable matter and other contaminants, points on the cumulative size-frequency curves were reproducible to 0.05 phi units.

Other data collected at drift stations included bottom-grab and gravity-core samples. Current velocity and direction were determined by keeping the ship next to the drogue and fixing the drogue's location by means of a pelorus at 15-minute intervals.

Anchor stations were occupied at night. Surface-current velocity and direction were determined at 5-to-15-minute intervals by means of an Ekman-Merz Current Meter. Other anchor-station measurements were the same as those taken on a drift station.

In addition to the survey from the R/V Shimada, the Rio Congo tidal flat and the tidal creeks draining the mangrove forests of the lower Rio Congo were reconnoitered from a 5-m launch. Aerial reconnaissance was conducted from a plane rented in Panama City, and aerial photographs were obtained from the Panama Geological Survey.

Physiography and Hydrology. The Darien Isthmus of western Panama consists of a broad breached anticline whose core is occupied by a major southwest-flowing river, the Chucunaque River. In southeastern Darien, the Chucunaque turns southward, crosses the Pacific Coast range, and drains into the sea as the Rio Tuira (Fig. 2). The Gulf of San Miguel is the drowned lower valley of the Tuira.

The Gulf of San Miguel is an irregularly shaped body of water 30 km wide at the mouth. Its bedrock consists of steeply dipping low-grade metasediments and metavolcanics whose regional strike is parallel to the coast and at right angles to the estuary. The Gulf's irregular outline results from the interaction of the drainage system and the bedrock structure.

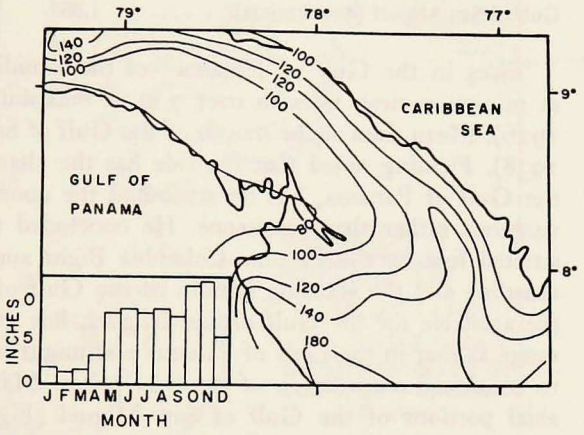

Figure 4. Isohyetal map of Panama and the monthly rainfall at the head of the Gulf of San Miguel.

Nearby hills rise to 1000 m. The marginal bays of the Gulf have flat floors less than 15 m deep, but the central channel reaches a depth of 36 m at the head of the Gulf. A detailed examination of one of the bays, Ensenada Pena Hueca (Hollow Rock Bay) indicates that the flat floor is the upper surface of a tide-maintained prism of mud overlying an irregular rocky floor (Fig. 3). The central channel of the Gulf of Panama was probably initiated by fluvial erosion during Pleistocene low stands of the sea, but its undulating thalweg is presently being kept open by tidal scour.

No direct determinations of river discharge are available for this little-frequented area. However, rainfall data are available and river discharge may be estimated from them. Mean annual rainfall ranges from 2000 to 3500 mm (about 80 to 140 inches) over the basins draining into the Gulf of San Miguel (Fig. 2). The rainfall is unevenly distributed, with a marked dry season from December through April (Fig. 4). Rating curves prepared on a two-year exceedance basis for the nearby Gatun Lake watershed have been used to estimate the fresh-water input of the Gulf of San Miguel (Table I).

An attempt has been made to weigh the values obtained for the mean annual rainfalls of the different basins. The results have order-of-magnitude validity at best and are useful only because no better data are available. The results suggest that the Tuira-Chucunaque discharge is by far the most important component, having a mean annual discharge on the order of 1×10^6 m^3.

Table I. Estimates of fresh-water flow into the Gulf of San Miguel.

Basin	Area (km^3)	Peak flow (m^3/sec)	Annual discharge (m^3)
Tuira-Chucunaque	11,158	8.0	1×10^6
Northern coastal rivers	901	2.0	2×10^3
Southern coastal rivers	1,841	3.0	4×10^4
Gulf of San Miguel (direct rainfall)	1,065	170 mm/day	2×10^3

Tides in the Gulf of Panama—of the semidiurnal type—vary from 2 m at minimum neap tides to over 7 m at maximum spring tides (Kirkpatrick 1926). Mean tides at the mouth of the Gulf of San Miguel are 4 m (Fleming 1938). Fleming noted that the tide has the character of a standing wave in the Gulf of Panama, but he attributed the anomalously high range to convergence rather than resonance. He concluded that the tidal prism is constricted first by the Panama-Colombia Bight and further by the converging coastline and the shoaling bottom of the Gulf of Panama. No accurate data are available for the Gulf of San Miguel, but the tide clearly has as great a range as that in the Gulf of Panama and might be expected to be greater due to continued constriction of the tidal prism. Maximum tidal currents in the axial portions of the Gulf of San Miguel (Fig. 5) average 200 cm/sec on the flood tide and 230 cm/sec on the ebb tide (approximately 3.4 and 3.6 knots respectively).

The structure of the water in the Gulf of San Miguel corresponds to the moderately stratified estuary of Pritchard (1967). The lower and central Gulf is weakly stratified; in summer, surface salinities are 26 to 30 while surface temperatures are close to 29°C; bottom salinities and temperatures are 2 to 3 units lower (Figs. 6, 7, 8). Fig. 7 shows that, at the mouth of this Gulf, the vertical salinity range in parts per thousand numerically overlaps the vertical temperature range in degrees centigrade. Toward the head of the Gulf, the salinity curve shifts toward lower values but retains its characteristic shape until the tributary estuaries are reached (Fig. 8A, 8B). As the tide begins to flood, these basins are filled with a mosaic of nearly homogeneous water masses separated by strongly stratified zones, marked at the surface by lines of flotsam. However, as the current velocity increases and the tide begins to move over the shoals rather than between them, the water masses begin to loose their identity due to turbulent mixing generated by irregular bottom topography. Note in Fig. 8B that the isopleths for temperature and salinity are irregular to nearly vertical as the tide moves over the bar at the mouth of the Rio Congo. At this time, large-scale turbulence in the form of surface slicks, boils, and eddies could be observed. As the turbulently mixed water rode over the denser water in the scour hole behind the bar, stratification was resumed. By high tide, the salinity fronts had advanced approximately 10 km up the tributary estuaries, which were then filled with weakly stratified and relatively homogeneous water.

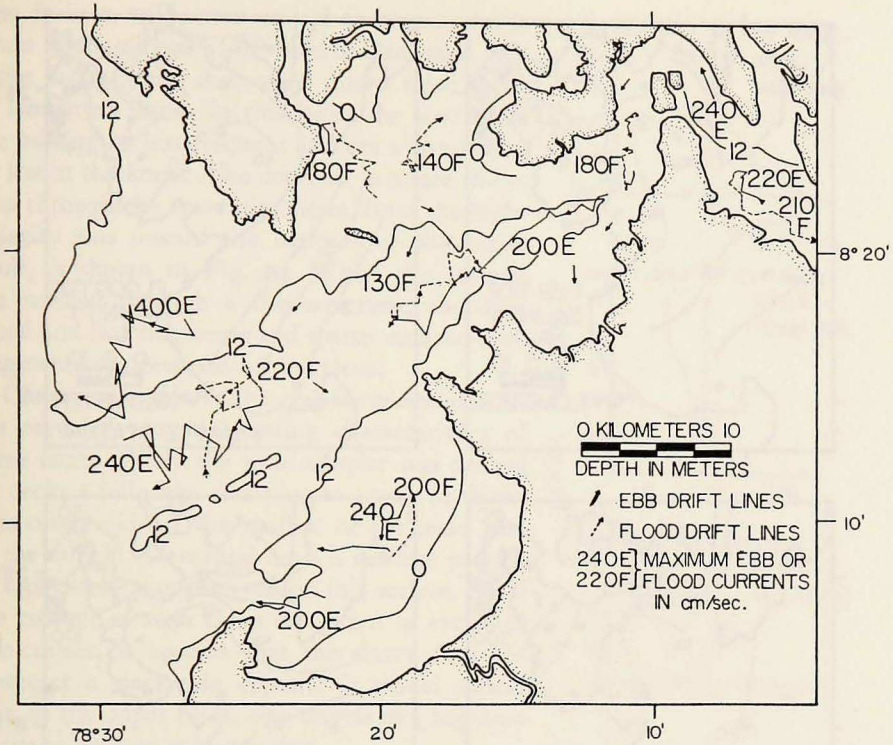

Figure 5. Drift stations, with maximum tidal current indicated for each major line. Anomalously high value on the Banco Del Buey (400 cm/sec) may be in error or may represent a vortex during interaction of the ebbing Gulf water and the north-flowing Panama current.

In the Tuira estuary, further mixing occurs when the water mass passes out through the high-velocity conduit of Boca Grande. Although this passage reaches depths of 40 m, turbulence extends from top to bottom at midtide. At such times, the velocity attains 250 cm/sec (approximately 4 knots) and the surface is distorted by large "boils" of rising water. It seems probable that the tide ebbing from Boca Grande spreads out over the center of the Gulf as a plane jet, slowly entraining subjacent layers and initiating the weak stratification in the central and lower Gulf. The scour hole at the mouth of the Rio Congo seems to play a similar role as a mixing mechanism for Rio Congo water.

It appears then that, within the Gulf of San Miguel, the primary interfaces between fresh and salt water occur in the tributary estuaries where they are most clearly defined during the beginning of flood tide. Specific examples are documented in Fig. 8.

Bottom Sediments. Facies of the Upper Gulf. Bottom sediments in the Gulf of San Miguel may be divided into six facies, primarily on the basis of

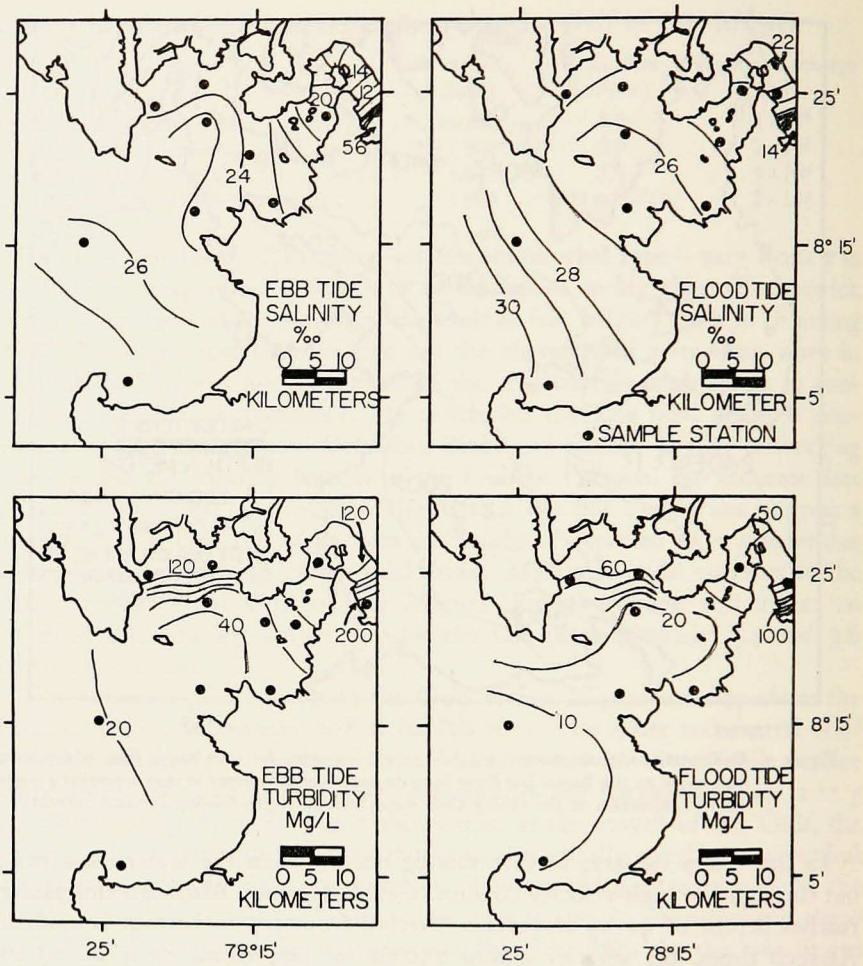

Figure 6. Salinity and turbidity data, collected during the period 7/II/67–7/XII/67. Stations occupied within a half hour of slack water.

texture and secondarily on the basis of primary structures and color, as indicated in Fig. 9. In the Tuira Estuary and upper Gulf of San Miguel, facies are symmetrically disposed about the bathymetric (and hence current-velocity) axis of the Gulf. The axial facies is a very fine-grained to medium-grained well-sorted moderate-brown sand (5 YR 4/4, National Research Council Rock Color Chart), with a patchy distribution. Grab samples reveal cross stratification and portions of sand waves having amplitudes of up to 15 cm. These sand patches are set in a matrix of the second facies: dark-yellowish brown (5 YR 4/2) to medium-dark gray (N 4) lutite (silt plus clay) interbedded with the moderate-brown sand. The strata, as revealed in cores, range in thick-

ness from a millimeter or less to 10 cm; lutite strata predominate. The interbedded sand and lutite facies grade shoreward into a third facies of laminated lutite; in this facies the sand strata are missing or less frequent and are a centimeter or less in thickness. The decrease in strata thickness through the two lutite facies, from the high-velocity axis toward the margins of the upper Gulf, is shown in Fig. 10. When the samples are washed through a 6-mm screen, abundant wood and leaf fragments and sparse mollusc-shell fragments are retained on the sieve.

Close observation of the grab samples and cores has revealed some interesting characteristics of these facies. When the grab sampler was opened on deck, a jelly-like slurry up to 10 cm in thickness often slid off the surface of the main part of the sample. In several cases a delicate pattern of tool marks was observed on this surface. Since the current at such times was often in excess of 200 cm/sec, it appears that the slurry does not represent a slack-tide deposit. It would appear that, in the upper Gulf, clay travels as a bed-load slurry as well as in suspension.

A second type of clayey bed load observed in grab samples in the upper Gulf consisted of masses of rounded gravel-sized clay wafers overlying the cohesive lutite of the main sample. These were most common in the interbedded sand and lutite facies; no doubt they represent lutite beds torn up during periods of maximum tidal current.

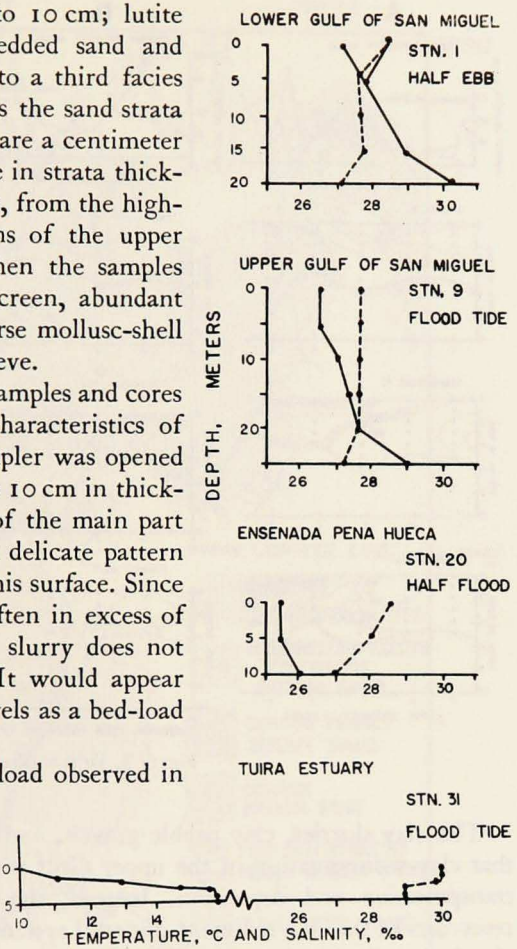

Figure 7. Temperature and salinity profiles. Flood-tide stations occupied within 30 minutes of high water. Descending order of graphs is from mouth to head of estuary. Solid lines are salinity in ppt, dashed lines are temperature in °C. Abscissa may be read in either unit.

Where clay wafer gravels occurred over the laminated lutite facies, the wafers and the underlying lutite tended to be medium-dark gray rather than the more common moderate-yellow brown. Where these two color phases occur in the same core, the moderate-yellow brown overlies the medium-dark gray, with a sharp contact between them. Percent-water determinations on one such core (PC 54, Fig. 11) indicate that the brown clay is over 60% water while the gray clay is less than 50%: hence the gray clay is old and compacted and the contacts are local disconformities.

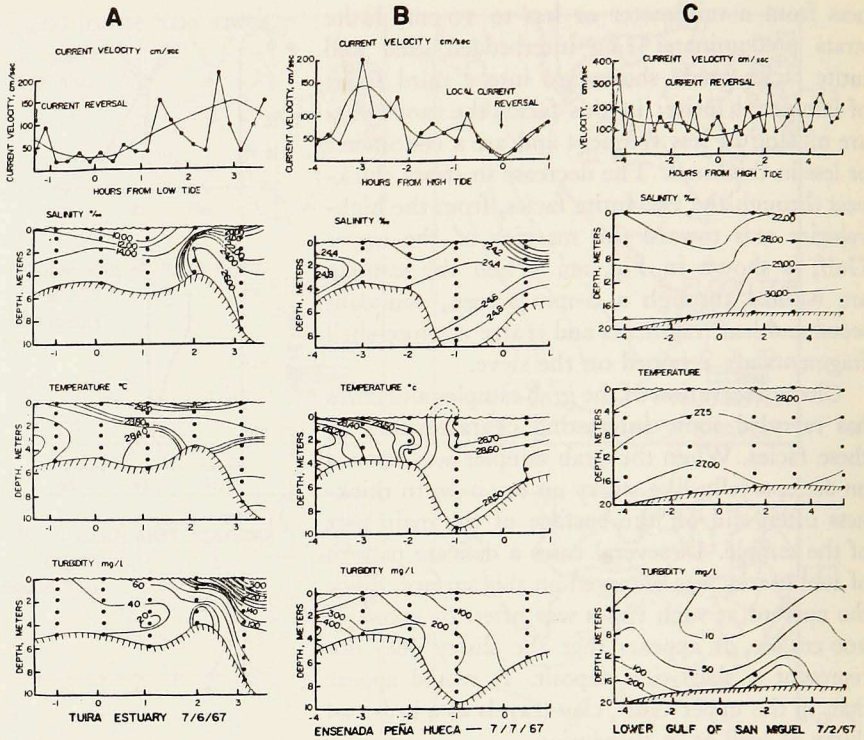

Figure 8. Drift-station data.

The clay slurries, clay pebble gravels, and internal disconformities indicate that clay sedimentation in the upper Gulf is not simply a two-step process of transportation and deposition. Instead, the marginal lutite facies serve as reservoirs in the fine sediment-dispersal system (see *Suspended Sediments*). The clay is deposited and resuspended many times before it escapes from the Gulf. Residence times of clay particles in these reservoirs may range from a single tidal cycle in the case of the slurry to the unknown period of time necessary to compact clay and reduce its water content to less than 50%. The residence time of the gray clay may be centuries. It is not possible, therefore, to establish a chronology in the cores by estimating the present rate of deposition and then extrapolating backward, even if a compaction correction were introduced. Successive sand-clay couplets may represent half tidal-cycle deposits (Reineck, personal communication), but they are grouped into strata sets whose bounding surfaces are disconformities. Since the short-term sedimentation rate is high (3 m of clay were deposited on the Rio Congo tidal flat in one tidal cycle), the missing strata represented by the disconformity are probably of a much greater volume than the surviving sets.

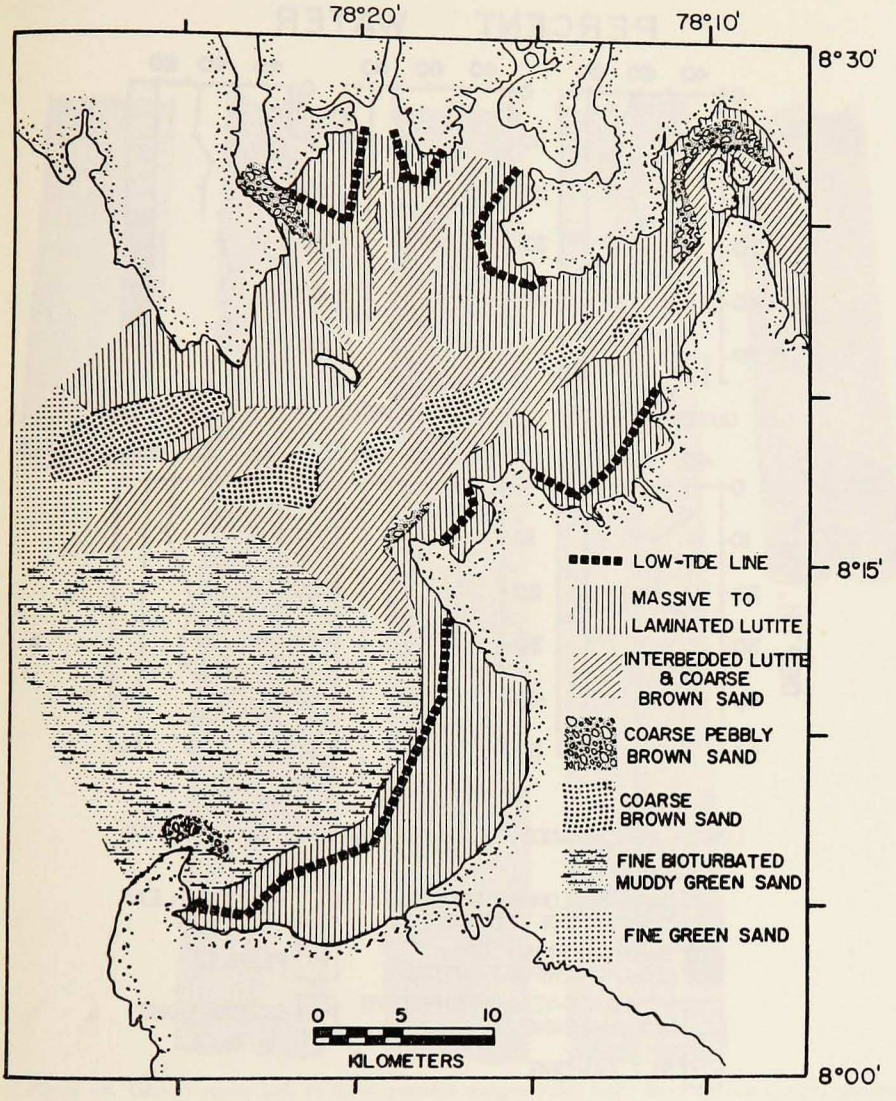

Figure 9. Bottom facies.

The laminated lutite facies extends into the intertidal zone without an obvious change in the character of the sediment. The water content (Fig. 12) and grain size of the constructional tidal flats in the upper Gulf result in a sediment of such a consistency that it will not support the weight of a man until he sinks in up to his thighs. Sediment of this consistency does not develop a meandering tidal channel-interfluve topography. The Rio Congo tidal flat

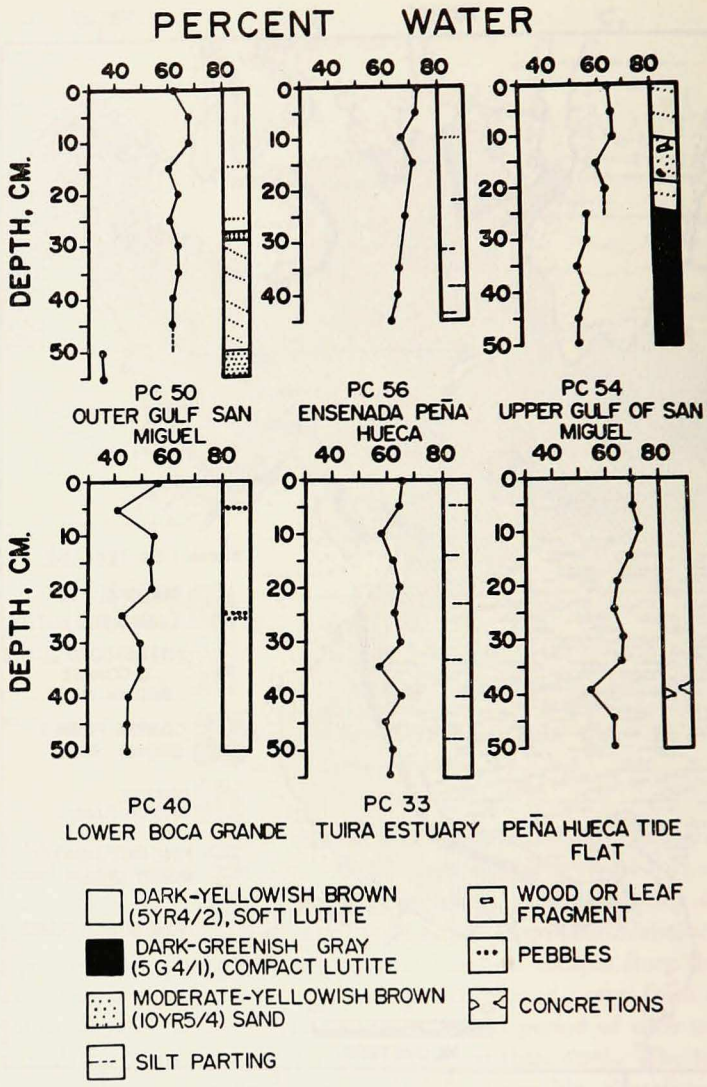

Figure 11. Water content of gravity cores.

of Ensenada Pena Hueca was examined in some detail (Fig. 3); it is about 10 km² in extent. It exhibits a relief of 4 m, but the slopes are never more than a few degrees; this is instead a swale and shoal topography. Reworking of the tidal flat is due to vertical erosion and deposition rather than by lateral migration of tidal channels. Reworking, however, is an important process, as evidenced by a peculiar feature at St. C on the Rio Congo flat (Fig. 3). Here

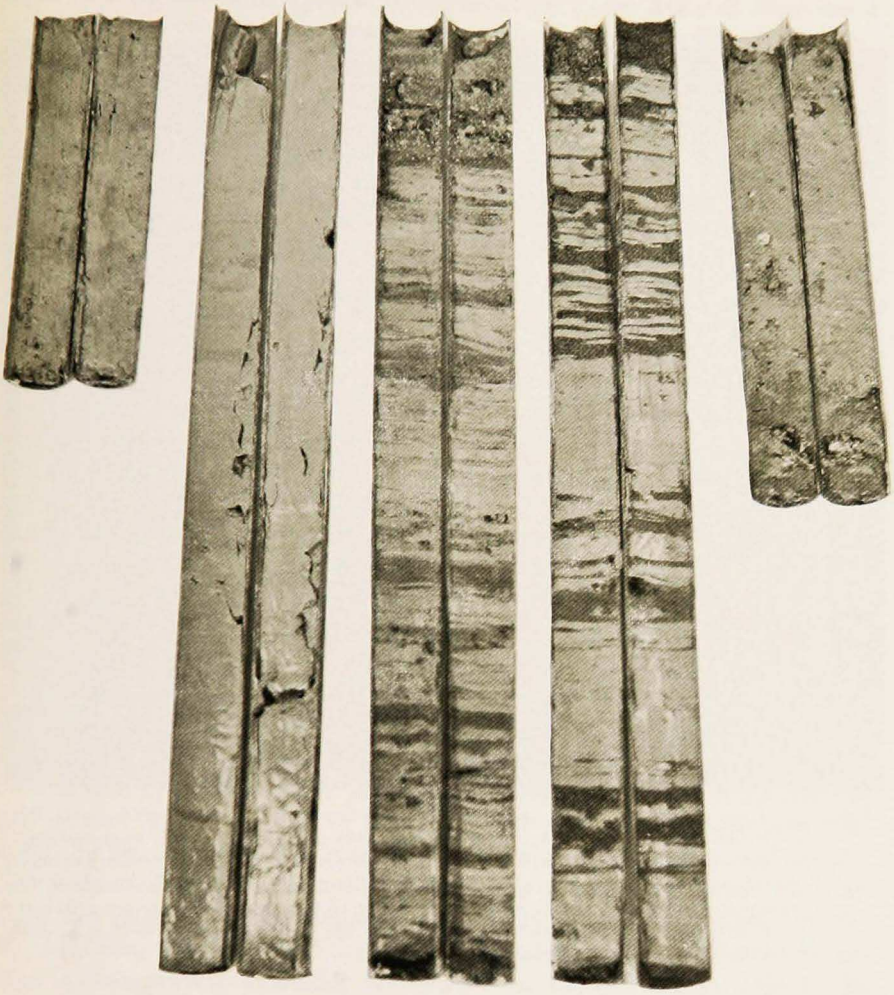

Figure 10. Gravity cores. Left to right: mottled mangrove-flat lutite from the Rio Congo; massive tidal-flat lutite from the Rio Congo tidal flat; very thin-bedded lutite and sand from the Gulf; thin-bedded lutite and sand from the upper Gulf; shelly and muddy bioturbated sand from the lower Gulf.

Figure 12. Aerial photograph of Isla Iguana Shoals, on western side of mouth of Ensenada Pena Hueca. North at top of photo. Tide flooding from west to east. Lower margin of turbid zone approximately a 10-m isobath. In lower center of picture, note turbidity streamers extending from submarine shoals downcurrent into the main turbid water mass. Note repeated comblike structure with "teeth" pointing upcurrent. Structure presumably due to large-scale rhythmic turbulence generated as tide swept up over threshold of Ensenada Pena Hueca. Altitude, 1000 m.

we discovered a concretionary pavement 1 m beneath the sediment surface. On recovery, these concretions proved to be encrusted with bryzoa on their upper surfaces and were riddled with numerous worm holes in their lower surfaces. Some concretionary masses were aggregates of broken sharp-edged pieces recemented together. We concluded that these concretions had formed and had been exhumed by tidal scour, after which they were encrusted with bryzoa, transported, fragmented, recemented, and finally reburied to the depth at which we found them.

Three additional facies of the upper Gulf are (i) a pebbly phase of the lutite facies in channels and near bedrock islands, (ii) intertidal clays of the fringing mangrove forest, and (iii) beach sands. The mangrove-flat clays are equivalent to the salt marshes of high latitudes. These clays are a medium bluish gray (5B 7/1), root-mottled with moderate-yellowish brown (10YR 5/4), and are dense (50% by weight or less water) enough to support a well-defined tidal-creek topography. Discontinuous beach sands occur at the high-water line, where the gradient is steep and where there is considerable fetch and high-tide wave activity. Where the fetch is small and the gradient steep, as in the Tuira Estuary, the margin is a river bank; where the fetch is small and the gradient gentle, a mangrove flat has built out, as around the margins of Ensenada Pena Hueca.

Facies of the Lower Gulf. The lower Gulf of San Miguel, consisting of Ensenada de Garachine, Banco Del Buey, and the channel between them, has a pattern of facies that is very different from the bilaterally symmetrical distribution in the upper Gulf. The most extensive facies is a dark-greenish gray (5 GY 4/1) very fine-grained to medium-grained shelly muddy sand. The mud (silt plus clay) content ranges from 15 to 30% by weight. Shell debris ranges from 0 to 12% by weight. When a sample was washed through a 6-mm screen, wood and leaf particles were abundant though subordinate to shell debris. While the ratio of living to dead mollusc shells was very low, several living molluscs could usually be found after washing a 0.2 m^3 sample. The fraction that was coarser than 6 mm was examined by James McLean of the Los Angeles County Museum and by Myra Keen of Stanford University. McLean, who identified the gastropods, stated that the molluscan assemblage is characteristic of muddy bottoms in the Panama region. Due to the coarse nature of the sieve, the finer forms, which comprise the bulk of such assemblages, were lost. X-radiographs of cores indicate that the dominant primary structure of this facies is a pervasive bioturbation mottling.

Two sand facies are present on the Banco Del Buey. The seaward facies consists of a very fine-grained and well-sorted dark-greenish gray (5 GY 4/1) sand. Its median diameter increases uniformly from 3.8 to 3.2 phi toward the crest of the shoal, suggesting that it is adjusted to a hydraulic regime of shoaling waves. A third Gulf facies occurs toward the crest of the shoal, where the median diameters increase abruptly to a range of 0.8 to 1.9 phi. Samples

consist of a coarse moderate-brown shelly sand, with shell fragments comprising up to 20% by weight. This facies lies in 2 to 4 m of water, where turbulence due to wave refraction is intense. The present hydraulic regime is perhaps adequate to explain its characteristics. However, the texture and color of this facies may indicate a relict origin.

Two other facies are of note in the lower Gulf. A marginal lutite facies occurs between Banco Del Buey and the mainland. Another occupies the intertidal zone of the Ensenada de Garachine. This second lutite zone is anomalously silty; the median diameters are 4 to 6 phi versus the 8-phi characteristic of the upper Gulf lutites. Peculiar sand ridges occur in the upper intertidal zone of Ensenada de Garachine; they are bilaterally symmetrical ridges normal to shore. Their triangular cross sections are estimated to be 10 by 3 m, and their length is as much as 90 m.

The following characteristics of the lower Gulf facies serve to distinguish them from the upper Gulf facies: (i) Loss of well-defined axial symmetry of facies distribution, (ii) reduced sedimentation rate as indicated by bioturbation, and relative abundance of shell hash and living molluscs, and (iii) a reduced importance of lutite facies, indicating a reduced suspended sediment supply.

The texture and composition of the upper Gulf facies reflect the high rate of supply of lutite, and their distribution reflects the powerful rectilinear tidal regime. The lower Gulf facies are relatively impoverished in lutite, due in part to dilution of the ebbing upper Gulf water by the northward-flowing Panama current and in part because the upper Gulf serves as a hydraulic trap for suspended sediment. The upper Gulf is clearly an estuarine sedimentary environment while the lower Gulf is more nearly a shelf environment. The distinction may be one of sediment source as well as of hydraulic factors; the greenish-gray sands of the lower Gulf contrast strongly with the moderate-brown estuary sands, and they may be shelf-derived.

Clay Mineralogy. The mineralogy of the less than 2-μ fraction of 15 bottom-sediment samples was determined by X-ray diffraction analysis. The samples were selected according to geographic position and according to the major sedimentary environment (central channel or marginal bay). Untreated and glycol-solvated sediments were examined by X-ray diffraction. The untreated clay-sized fraction produced either a poor X-ray pattern or none, suggesting that the clays exist naturally as greater than clay-sized floccules rather than as discrete particles. The sediments were also treated and X-rayed after the techniques described by Pirie (1967); the analyses followed the procedure of Johns et al. (1954). The amounts of illite, kaolinite, chlorite, and montmorillonite in each sample are listed in Table II. Fig. 13 illustrates the areal distribution of the clay minerals and Fig. 14 illustrates the relative proportions of illite, kaolinite, and montmorillonite. Chlorite is present in less than half of the bottom sediments examined and is not included in Fig. 13.

Table II. Color and clay mineral analyses of bottom sediments, Bay of San Miguel.

Sample no.	Color code*	Color name	Illite†	Kaolinite	Chlorite	Montmorillonite	Percent of clay
P-1	10 YR 4/2*	Dark-yellowish brown	1.8†	0.9	1.8	4.5	41
P-7	10 YR 5/4	Moderate-yellowish brown	3.6	1.8	0	3.6	9
P-8	5 YR 7/2	Yellowish grey	4.8	1.2	1.4	1.7	61
P-9	10 YR 4/2	Dark-yellowish brown	4.1	4.1	0	0.9	50
P-14	10 YR 4/2	Dark-yellowish brown	1.2	0	7.8	0	55
P-20	10 YR 4/2	Dark-yellowish brown	3.6	3.6	0	1.8	68
P-24	10 YR 5/4	Moderate-yellowish brown	1.9	0	4.7	2.4	70
P-27	10 YR 4/2	Dark-yellowish brown	0	0	0	9.0	44
P-29	10 YR 4/2	Dark-yellowish brown	3.8	1.9	0	3.4	48
P-30	10 YR 6/2	Pale olive	2.2	2.6	0	4.1	71
P-34A	10 YR 4/2	Dark-yellowish brown	2.9	2.2	1.4	2.3	52
P-51	5 YR 5/2	Light-olive gray	0.8	0.8	6.6	0.9	02
P-59	10 YR 4/2	Dark-yellowish brown	0	0	0	9.0	41
P-62	5 Y 5/2	Light-olive gray	3.9	1.2	1.2	2.7	02
P-66	10 YR 4/2	Dark-yellowish brown	0	0	0	9.0	06

* Code of Munsell Soil Color Chart.

† Parts in ten, assuming 10% is not recorded on the diffractogram.

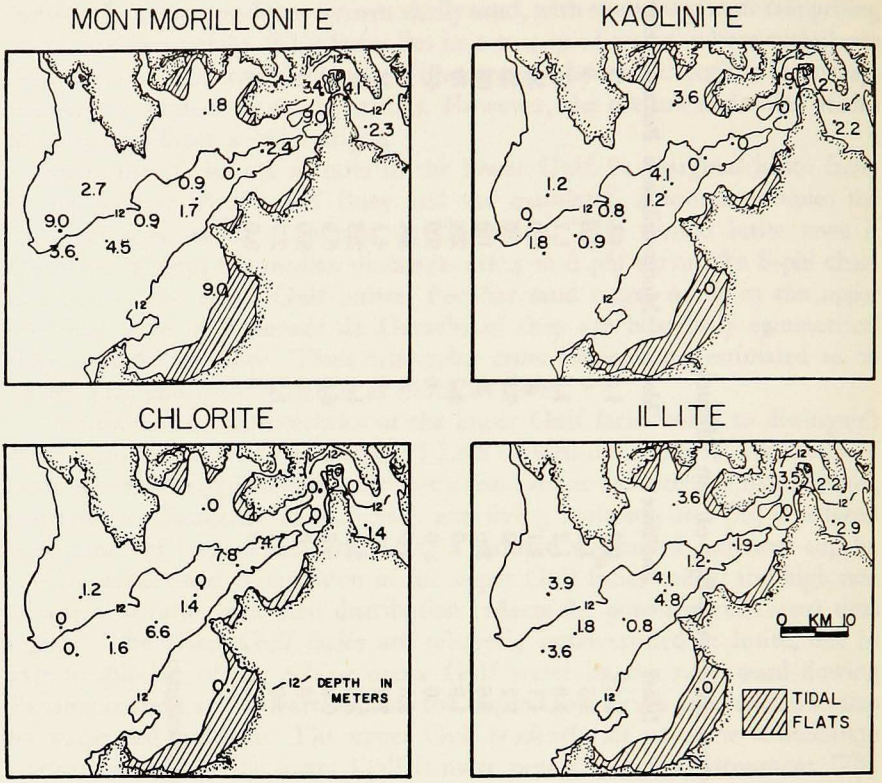

•1.2 = SAMPLE STATION AND ABUNDANCE OF CLAY (PARTS IN TEN)

Figure 13. Clay mineral abundances (parts per ten).

In the Gulf of San Miguel, illite is the most uniformly distributed of the major clay minerals. It is most abundant in the central Gulf (mean of five samples, 3.1 parts in ten), next most abundant in the lower Gulf (mean of six samples, 2.3 parts in ten), and least abundant in the upper Gulf (mean of four samples, 2.2 parts in ten). Randomly mixed layers of 10 and 17.70 Å are abundant and may reflect the weathering of detrital illite.

Kaolinite is more abundant in the upper and central Gulf (0 to 4.1 parts in ten) and less abundant in the lower Gulf (0 to 1.2 parts in ten).

Chlorite is absent or nearly absent from most of the 15 samples examined. It is most abundant (1.8 to 7.8) in the channel of the central Gulf and is lacking or low in abundance (0 to 1.4 parts in ten) in the upper Gulf, in the marginal bays, and in the channel of the lower Gulf.

The montmorillonite distribution is bimodal; it is relatively abundant in the upper Gulf (2.3 to 9.0 parts in ten) and in the lower Gulf (2.7 to 9.0 parts in ten) and less abundant in the central Gulf (0 to 2.4 parts in ten).

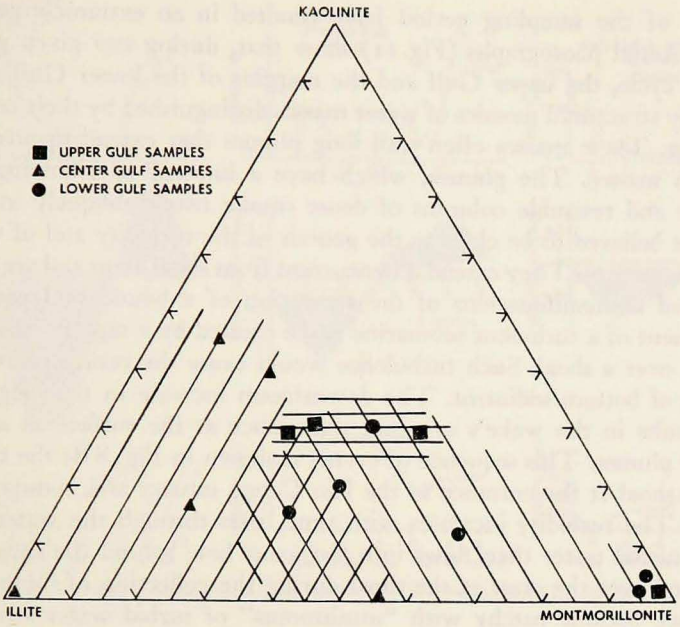

Figure 14. Percent illite, chlorite, and kaolinite in bottom samples.

Regularly interstratified vermiculite and mica occurred in one sample (P-9).

The pattern of the clay-mineral distribution (Figs. 13, 14) is compatable with the pattern attributed by Whitehouse et al. (1960) to size sorting and differential flocculation, since (i) the upper Gulf is relatively kaolinitic, (ii) 3-layer clays are relatively abundant in the central and lower Gulf, and (iii) the lower Gulf is specifically enriched with montmorillonite. According to Whitehouse et al. (see also van Andel and Postma 1954, Pryor and Glass 1961), kaolinite tends to settle out before other clays because of its coarser grain size and montmorillonite settles last because of its very fine grain size. This physical sorting is believed to be strongly reinforced by chemical behavior; experiments (Whitehouse and Jeffrey 1955) have shown that the flocculation of kaolinites and illites is completed mainly at very low chlorinities while the flocculation of montmorillonite increases gradually with increasing chlorinity. Unfortunately, our sample density is not sufficient to validate this model. The pattern in the Gulf of San Miguel could also be described as an inadequately sampled random distribution with a high variance.

Suspended Sediments. TURBIDITY. The flood-tide and ebb-tide turbidity distribution in the Gulf of San Miguel is shown in Fig. 6. Recorded turbidities range from 0.10 to 200 mg/l. The low density of the sample net and the 10-day

duration of the sampling period have resulted in an extremely generalized picture. Aerial photographs (Fig. 11) show that, during any given portion of the tidal cycle, the upper Gulf and the margins of the lower Gulf consist of intricately structured mosaics of water masses distinguished by their contrasting turbidities. These masses often trail long plumes that extend upcurrent from the main masses. The plumes, which have a knotted or billowing internal structure and resemble columns of dense smoke rising obliquely in a strong wind, are believed to be clues to the genesis of the turbidity and of the water masses themselves. They extend downcurrent from shoal areas and are therefore interpreted as manifestations of the separation of a boundary layer and the development of a turbulent submarine wake created by a rapidly moving sheet of water over a shoal. Such turbulence would cause the resuspension of large amounts of bottom sediment. The downstream increase in the height of the wake results in the wake's eventual appearance at the surface as a series of turbidity plumes. This sequence of events is shown in Fig. 8B; the tide floods over the shoal at the entrance to the Rio Congo estuary and is mixed by turbulence. The turbidity increases with time, rises through the water column, and the turbid water then flows into the scour hole behind the shoal. As the ship passed over the crest of the shoal during the collection of these data, the sea surface became patchy with "mushrooms" of turbid water separated by clearer areas.

Downstream the eddies slowly merged and decayed; the plumes became a homogeneous water mass, having a sharply defined front at the edge of the adjacent water mass and poorly defined flanks. Where sharp boundaries existed, they could be identified from shipboard by the contrasting turbidity and by the presence of foam lines containing floating wood and seaweed. As noted, the identity of these water masses depends primarily on the salinity- and temperature-defined density differences. Even very turbid water will override clear water if the former is less saline (Fig. 8C). In some cases (Fig. 11), turbidity variations within the water masses reveal several orders of large-scale rhythmic instability similar to the rippled patterns seen in clouds.

An analysis of the turbidity data and of the aerial photographs indicates that the 12-m isobath is a critical one for the generation of turbid water. Shoaler water consists of poorly to sharply defined water masses, with turbidities ranging from 60 to 200 mg/l. Deeper water in the center of the Gulf has turbidities ranging from 10 to 40 mg/l. As the absolute turbidity decreases, the relative organic-carbon content of the suspended material increases to 80%, dry weight. Such samples, when flushed from the centrifuge, are a vivid green and have the distinctive odor of algae; hence the turbidity of the deeper water is largely biogenic.

It is clear that, in the Gulf of San Miguel, turbidity maxima occur within poorly defined to well-defined water masses that result from water flowing at velocities of 100 to 200 cm/sec over shoals 12 m or less in depth. The

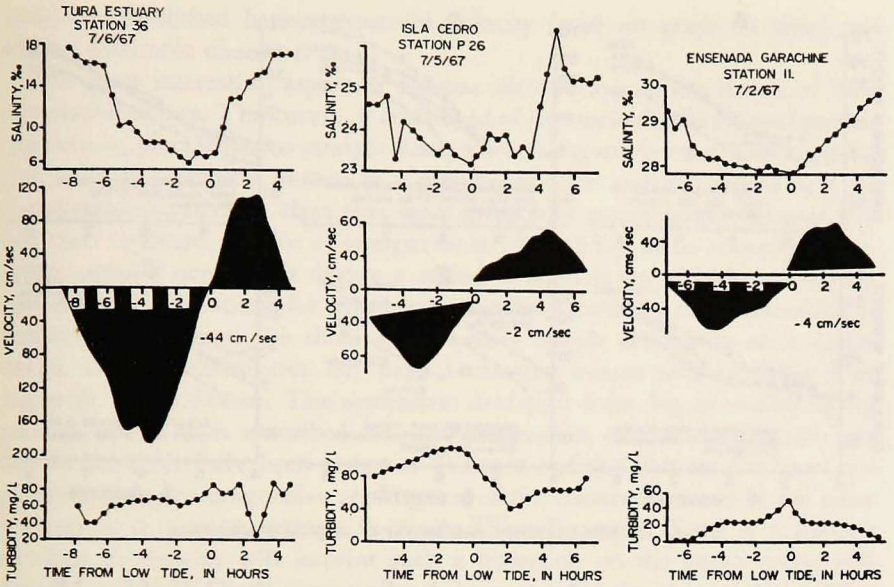

Figure 15. Surface data for anchor stations. Negative (ebb) residual currents indicated beside current-velocity plots.

relationship between current velocity and turbidity is shown in the Rio Congo and at the lower Gulf drift stations (Figs. 8 A, 8 B). Here the time of maximum turbidity on the bottom closely correlates with the time of maximum current. In extremely shallow water (less than 3 m) there may be an apparent inverse relationship between turbidity and current velocity (Fig. 15). Actually, the time of greatest turbidity is depth-dependent rather than current-dependent in such cases; at low tide, the surface is so close to the bottom that turbidity is high, even though the current is slack.

Size Distribution. A size analysis of clays has heretofore been performed mainly as an adjunct to whole-sample analysis of bottom sediments. An analysis is commonly performed by pipetting, by hydrometer, or by electronic methods (Coulter Counter). The clays are dispersed with a peptizing agent prior to analysis. The results of such analyses accurately reflect the reaction of the clay to the peptizer but bear little relationship to the size distribution of the clay during deposition.

It seems reasonable to assume that the size distribution of clay floccules is a major control in the sedimentation of suspended fine sediments in coastal waters, just as particle size is a control in the sedimentation of sand-sized particles. Using the techniques and equipment described previously, we have conducted *in situ* size-frequency measurements of the hydraulic diameter of suspended sediments in order to test this hypothesis. The results of the analyses are presented in Fig. 16.

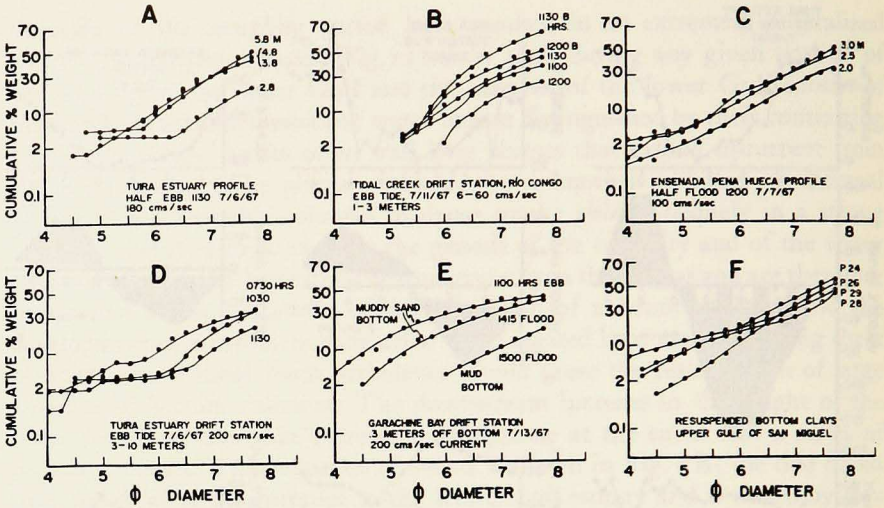

Figure 16. Size-frequency distribution of suspended sediments.

The analyses show that the suspended sediments in the Gulf of San Miguel have generally similar distributions in the observed range (silt class; 4 to 8 phi). Irregularities in the coarse end of the curves were caused by large low-density plant fragments that are hydraulically equivalent to silt.

The curves were recalculated to 100% so that inclusive graphic parameters could be determined (Folk and Ward 1957). The results show that the size-frequency distribution curves become more peaked (have higher kurtosis) and become skewed toward the fine side of the distribution as the mean grain size increases. The standard deviations of the distributions decrease as the mean grain size increases. These trends are thought to indicate the mixing of two log normally distributed populations: (i) a subordinate coarse population of quartz grains and plant fragments, and (ii) a dominant fine population of clay floccules.

Size analysis of vertical profiles of suspended sediments reveals an increase in median diameter (shift of curves to left) with depth, as predicted by Brush (1965); see Figs. 16A, 16C.

The median hydraulic diameter of suspended sediments at a given depth varies with time as a function of current intensity, in a manner dependent on total water depth. In water deeper than 3 m, the sediment was coarsest when the current was fastest and decreased (curves shift to right, see Fig. 16D) in coarseness as the current waned. In water shoaler than 3 m, the reverse relationship prevailed. As in the case of sediment concentration in shoal water, the bottom at low water is so close to the surface that the median diameter of the suspended sediment is high, even though the current is nearly slack. This reverse relationship was observed only at anchor stations; at drift stations (Fig. 16B) the boat drifted over areas of varying depth so that no relationship

could be established between current velocity (read on graph as time) and median hydraulic diameter.

The most interesting aspect of the size distributions is the shapes of their cumulative curves. The curves, if comprised of log-normally distributed particle populations, should plot as straight lines, since the graph is essentially a log-log plot, with the ordinate plotted as a probability scale and the abcissa as a phi transformation. Bottom clays that were artificially resuspended on board ship and then analyzed do plot as straight lines (Fig. 16 D), as do suspended sediments sampled over shoals during a period of accelerating tidal currents (Fig. 16 D). Size distributions for other stations where currents are decelerating in deeper water beyond the shoal are generally simple convex-up arcs. Other curves are convex-up arcs but have horizontal coarse tails resulting from vegetable contaminants. The systematic deviation from log normality of the arcuate segments is described as *coarse truncation* of the distribution; the coarser floccules have been removed (Tanner 1964). This results from *progressive sorting* or progressive settling out of the coarser fractions as the effectiveness of a waning current decreases (Russell 1938). Even a temporary decrease in velocity will imprint such a distortion on the curve unless subsequent velocity is sufficiently intense to overcome the "scouring lag" and resuspend the lost fractions.

The hydraulic diameter of clay floccules should also vary with salinity, temperature, EH and pH, and concentration (Ippen 1966); and it should vary with current velocity because faster currents are more effective with greater turbulence. Faster currents increase the rate of floccule collision and therefore the rate of floccule growth (Ippen 1966). This relationship should pass through a maximum value as extremely turbulent waters begin to tear the fragile floccules apart. None of these additional relationships was observed, possibly because our methods of data collecting were not capable of resolving them.

Fine-sediment Dispersal. The Gulf of San Miguel displays a system of fine-sediment dispersal in which there are two types of components: (i) water masses containing suspended fine sediment, and (ii) lutite bottom deposits that exchange material with the overlying water masses. These bottom deposits are present throughout the area studied. In the lower Tuira Estuary, the main channel is a narrow passage close to the north shore; the rest of the estuary is a mud shoal less than 2 m in depth. In the Gulf proper, the mud prisms in the marginal bays extend from the edges of the main channel into the intertidal zone and into the mangrove flats. The most voluminous mud prism is the one occupying Ensenada Pena Hueca (Fig. 3).

In the last decade there have been numerous studies of the hydraulic mechanisms that govern fine-sediment dispersal in estuarine systems; these have been reviewed by Postma (1967). Salinity stratification, documented by us in

the Gulf of San Miguel, is responsible for maintaining in estuaries a concentration of high suspended sediment against the turbidity gradient; that is, in such estuaries the zone of stratified water is commonly more turbid than either the incoming river water or the adjacent ocean into which the estuary water escapes. This turbidity maximum has been attributed to flocculation resulting from the mixing of fresh and saline water. Postma and Kalle (1955), however, have regarded the zone of stratification as more of an hydraulic trap than a chemical trap. They have suggested that the floccules in the upper seaward-moving brackish water sink into the salt wedge that carries them back upstream, only to feed them once more into the overlying brackish water. Thus particles may be recirculated many times before escaping, and a turbidity maximum is generated. Since the upper Tuira Estuary is uncharted and hazardous to navigation, we were not able to accurately map the turbidity maximum within the estuary. However, our salinity data (Fig. 6, 8, 15) suggest that the lower portion of this and other tributary estuaries comprises the most sharply stratified sectors of the system and that turbidity maxima are probably present. We suggest also that the 2-m shoal blocking the throat of the Tuira is generated by such a turbidity maximum. Such a shoal is in a state of dynamic equilibrium, with the turbid water mass oscillating back and forth above it. Thus sediment would pass from a state of deposition into suspension and back again during every tidal cycle.

Hydraulic mechanisms are also important in the accumulation of muds on tidal flats (Van Straaten and Kuenen 1958). The most significant are (i) the scour lag, (ii) the settling lag, and (iii) the time-velocity asymmetry of the nearshore tidal cycle. The scour lag refers to the fact that, due to the cohesive nature of mud and due to the hydraulic smoothness of mud surfaces, it takes a faster current to erode mud than to transport it. Thus, suspended fine sediment, which can be carried by swift offshore currents into marginal areas of reduced current velocity, is deposited and retained there because the erosion threshold is not exceeded. The settling lag refers to the fact that a flood tide advancing across a tidal flat will decelerate until it is no longer competent to carry a given particle, but the settling particle will be carried further shoreward until it reaches bottom. In this final position, a current capable of transporting the particle will occur, if at all, later in the cycle. Time-velocity asymmetry refers to the fact that, if a given water mass is followed, the period of maximum current velocity is displaced toward low tide, because the water mass, when spread over the tidal flat at high tide, is thinner and moves more slowly than when it moves through permanent water channels at low tide. Hence particles have a greater chance of settling out near shore at high slack water than at low slack water. For a more detailed discussion of these mechanisms, see Postma 1967.

Our data tend to confirm this concept of tidal-flat sedimentation elucidated in better-studied midlatitudinal water bodies. In addition, we have been able

to examine in some detail the scour portion of the tidal-sedimentation cycle. Our study has demonstrated that turbidity-generating bottom scour is the result of the development of a turbulent boundary layer when a tidal stream moves over a marginal flat. It has also demonstrated the sensitive response of the size-frequency distribution of suspended sediment to topography-induced fluctuations in velocity.

In the Gulf of San Miguel, then, both the nontidal estuarine circulation in the tributary estuaries and the hydraulic concentration in the marginal bays of the main Gulf generate turbidity maxima. These exist in a state of dynamic equilibrium with subjacent mud shoals whose surfaces are shaped by the interaction of midtide scour and slack tide deposition. However, the shoals experience a net gain of sediment, and the lutite facies of the bays, tidal flats, and mangrove forests are prograding toward the main channel. We presume that the process was initiated 7000 to 3000 years ago, when the post-Pleistocene sea-level rise underwent several decreases in rate (Russell 1967). Several kilometers of outbuilding have already transpired on the north shore of Ensenada Pena Hueca; this shore consists of a sheet of mangrove-covered lutite, with bedrock islands rising through it (Fig. 4). Ensenada de Garachine is likewise prograding, but it is less favorably sited for the reception of fine sediments. Its progradational plain consists of tidal-flat deposits overlain by a veneer of beach sand carried by longshore drift from adjacent premontories. Ultimately, the upper and central Gulf of San Miguel will lose its dendritic pattern inherited from the former river valley and will become a trumpet-shaped estuary in equilibrium with its tidal prism.

Acknowledgments. The project, of which this study is a part, was conducted by Frank Lowman, Head of the Marine Biology Program, Puerto Rico Nuclear Center. This study was made possible by his planning, logistical support, and technical advice. Field and laboratory assistance was rendered by Gregory Telek, Raphael Garcia, Catalina Lopez, and Miss Maria Negron. Special efforts by the ship's officer, Steven Walsh, and by the Captain and crew of the R/V SHIMADA, Puerto Rico Nuclear Center, permitted the accomplishment of a large amount of field work in a relatively short space of time.

We thank James H. McLean, Curator of Invertebrate Zoology at the Los Angeles Museum of Natural History, and Myra Keen of Stanford University for analyses of the molluscan fauna from the coarse fraction of the bottom sediments. We thank William W. Eden, Jr., Chief, Interoceanic Canal Studies Branch, Engineering Division, and Fred Able, of the same division, for hydrologic data from Darien Province. We also thank Lieutenant (j.g.) Froshure and Commander F. B. Cosby of Roosevelt Roads Naval Base, Puerto Rico, for supplying parachutes for drogues. Robert Jordan, University of Delaware, and Bruce Nelson, University of South Carolina, critically read the manuscript for us.

REFERENCES

Bradley, J. S.
1956. A simple turbidometer. J. sediment. Petrol., *26*: 61–63.

Briggs, L. I., and G. V. Middleton
1965. Hydromechanical principles of sediment structure formation, *In*, Primary structures and their hydrodynamic interpretation, pp. 5–16. G.V. Middleton, Editor. Spec. Publ., Soc. Econ. Petrol. Mineral., *12*; 265 pp.

Brush, L. M.
1965. Sediment sorting in alluvial channels, *In*, Primary structures and their hydrodynamic interpretation, pp. 34–52. G.V. Middleton, Editor. Spec. Publ., Soc. Econ. Petrol. Mineral., *12*; 265 pp.

Fleming, R. H.
1938. Tides and currents in the Gulf of Panama. J. mar. Res., *1*: 192–206.

Folk, R. L., and W. C. Ward
1957. Brazos River bar; a study in the significance of grain size parameters. J. sediment. Petrol., *27*: 3–26.

Ippen, A. T.
1966. Sedimentation in estuaries, *In*, Estuary and coastaline hydrodynamics, pp. 648–672. A. T. Ippen, Editor. McGraw-Hill, New York. 744 pp.

Johns, W. D., R. E. Grim, and W. F. Bradley
1954. Quantitative estimations of clay. J. sediment. Petrol., *24*: 242–251.

Jordan, R. R.
1965. Notes on techniques for sampling suspended sediment. S.E. Geol., *7*: 9–13.

Kirkpatrick, R. Z.
1926. Panama tides. Proc. U. S. nav. Inst., *52*: 660–664.

McKenzie, K. G.
1963. The adaption of a colorimeter for measuring silt-sized particles—a rapid photo-extinction (PE) method. J. sediment. Petrol., *33*: 41–48.

Pirie, R. G.
1967. Clay mineralogy of Bahia de Anasco, western Puerto Rico, *In*, Progr. Rep., Puerto Rico Nuclear Center, 1966, pp. 147–166. Frank Lowman, Editor. 374 pp.

Postma, H.
1967. Sediment transport and sedimentation in the estuarine environment, *In*, Estuaries, pp. 158–179. Amer. Ass. Advanc. Sci.; 757 pp.

Postma, H., and K. Kalle
1955. Die Entstehung von Trübungzonen im Unterlauf der Flüsse Speziell im Hinblick der Verhaltnisse in der Unterelbe: Dtsch. hydrogr. Ztg., *8*: 137–144.

Pritchard, D. W.
1967. Observations of circulation in coastal plain estuaries, *In*, Estuaries, pp. 37–44. Amer. Ass. Advanc. Sci.; 757 pp.

Pryor, W. A., and H. D. Glass
1961. Cretaceous-Tertiary clay mineralogy of the Mississippi Embayment. J. sediment Petrol., *31*: 38–51.

Russell, R. D.
1938. Effect of transportation on sedimentary particles, *In*, Recent marine sediments, pp. 32–47. P. D. Trask, Editor, Amer. Ass. Petrol. Geol.; 736 pp.

RUSSELL, R. J.
1967. Origin of estuaries, *In*, Estuaries, pp. 93–99. G. H. Lauff, Editor. Amer. Ass. Petrol. Geol.; 757 pp.

SIMMONS, GENE
1959. The photo-extinction method for the measurement of silt-sized particles. J. sediment. Petrol., *29*: 233–245.

TANNER, W. E.
1964. Modification of sediment size distributions. J. sediment. Petrol., *34*: 156–164.

VAN ANDEL, TJ. H., and H. POSTMA
1954. Recent sediments of the Gulf of Paria, *In*, Reports of the Orinoco Shelf Expedition, K. Nedrl. Akad. Wetensch. Verh., *20*: 42–56.

VOB STRAATEN, L. M. J. U., and PH. H. KUENEN
1958. Tidal action as a cause for clay accumulation. J. sediment. Petrol., *28*: 406–413.

WHITEHOUSE, V. G., and L. M. JEFFREY
1955. Peptization resistance of selected samples of kaolinitic, montmorillonitic, and illitic material, *In*, Clays and clay minerals, pp. 260–281. Proc. 7th. Natl. Conf. Clays, Clay Minerals. 269 pp.

WHITEHOUSE, V. G., L. M. JEFFREY, and J. D. DEBRECHT
1960. Differential settling tendencies of clay minerals in saline waters, *In*, Clays and Clay Minerals, pp. 1–79. Proc. 7th. Natl. Conf. Clays, Clay Minerals. 269 pp.